

Research Articles | Behavioral/Cognitive

The relationship between white matter architecture and language lateralisation in the healthy brain

<https://doi.org/10.1523/JNEUROSCI.0166-24.2024>

Received: 18 December 2023

Revised: 3 August 2024

Accepted: 26 September 2024

Copyright © 2024 Andrulyte et al.

This is an open-access article distributed under the terms of the [Creative Commons Attribution 4.0 International license](#), which permits unrestricted use, distribution and reproduction in any medium provided that the original work is properly attributed.

This Early Release article has been peer reviewed and accepted, but has not been through the composition and copyediting processes. The final version may differ slightly in style or formatting and will contain links to any extended data.

Alerts: Sign up at www.jneurosci.org/alerts to receive customized email alerts when the fully formatted version of this article is published.

The relationship between white matter architecture and language lateralisation in the healthy brain

Ieva Andrulyte^{1*}, Christophe De Bezenac¹, Francesca Branzi², Stephanie J Forkel³⁻⁵,
Peter N. Taylor^{6,7}, Simon S. Keller¹

¹ Department of Pharmacology and Therapeutics, Institute of Systems, Molecular and Integrative Biology, University of Liverpool, Liverpool, UK

² Department of Psychological Sciences, Institute of Population Health, University of Liverpool, Liverpool, UK

³ Donders Institute for Brain Cognition Behaviour, Radboud University, Nijmegen, the Netherlands

⁴ Brain Connectivity and Behaviour Laboratory, Sorbonne Universities, Paris, France

⁵ Centre for Neuroimaging Sciences, Department of Neuroimaging, Institute of Psychiatry, Psychology and Neuroscience, King's College London, London, UK

⁶ CNNP Lab (www.cnnp-lab.com), Interdisciplinary Computing and Complex BioSystems Group, School of Computing Science, Newcastle University, UK

⁷ Institute of Neurology, Queen Square, UCL, London UK

*Corresponding author:

Ieva Andrulyte

The BRAIN Lab, University of Liverpool Cancer Research Centre, 200 London Road, Liverpool, L3 9TA, UK

Email: ieva.andrulyte@liverpool.ac.uk

Authors' OrchIDs:

IA 0000-0002-8691-4078, CdB 0000-0002-2433-9776, FB 0000-0002-3780-9693, SJF [0000-0003-0493-0283](https://orcid.org/0000-0003-0493-0283), PT 0000-0003-2144-9838, SK 0000-0001-5247-9795

Running header: White matter asymmetries and language laterality

Keywords: white matter asymmetries, language lateralisation, tractography, connectometry, hemispheric asymmetries, MRI, corpus callosum, forceps minor

33

34 Number of pages: 25

35 Number of tables: 1

36 Number of Figures: 8 main figures and 2 extended figures

37 Number of words for abstract: 234

38 Number of words for significance statement: 101

39 Number of words of introduction: 630

40 Number of words for discussion: 1432

41

42 **Abstract**

43 Interhemispheric anatomical differences have long been thought to be related to
44 language lateralisation. Previous studies have explored whether asymmetries in the
45 diffusion characteristics of white matter language tracts are consistent with language
46 lateralisation. These studies, typically with smaller cohorts, yielded mixed results.
47 This study investigated whether connectomic analysis of quantitative anisotropy (QA)
48 and shape features of white matter tracts across the whole brain are associated with
49 language lateralisation. We analysed 1040 healthy individuals (562 females) from
50 the Human Connectome Project database. Hemispheric language dominance for
51 each participant was quantified using a laterality quotient (LQ) derived from fMRI
52 activation in regions of interest (ROIs) associated with a language comprehension
53 task compared against a math task. A linear regression model was used to examine
54 the relationship between structural asymmetry and functional lateralisation.
55 Connectometry revealed a significant negative correlation between LQs and QA of
56 corpus callosum tracts, indicating that higher QA in these regions is associated with
57 bilateral and right-hemisphere language representation in frontal and temporal
58 regions, respectively. Left language laterality in temporal lobe was significantly
59 associated with longer right inferior fronto-occipital fasciculus (IFOF) and forceps
60 minor tracts. These results suggest that diffusion measures of microstructural
61 architecture as well as geometrical features of reconstructed white matter tracts play
62 a role in language lateralisation. People with increased dependence on right or both
63 frontal hemispheres for language processing may have more developed

64 commissural fibres, which may support more efficient interhemispheric
65 communication.

66

67

68 **Significance statement:** The left cerebral hemisphere is dominant for language
69 functions in most people. In some healthy people, language functions are lateralised
70 to the right hemisphere or distributed across both hemispheres. The anatomy
71 underlying patterns of hemispheric language dominance are not well established.
72 Emerging evidence suggests that white matter connectivity and architecture is an
73 important feature of cortical functional organisation. In this work, we report that
74 people who have language functions distributed across both hemispheres have
75 greater inter-hemispheric connectivity compared to lateralised people. Our findings
76 provide further insights into the anatomical basis of language function and may have
77 wider clinical implications.

78

79 **Introduction**

80 It has long been hypothesised that grey matter asymmetries of regions that
81 support language function may be associated with functional lateralisation of
82 language in the human brain (Güntürkün et al., 2020). Associations between cortical
83 asymmetries and hemispheric language dominance (HLD) have been noted in some
84 studies of Wada-tested patients with epilepsy (Dorsaint-Pierre et al., 2006; Foundas
85 et al., 1996, 2002; Keller et al., 2018) and healthy controls who underwent structural
86 and functional MRI (Josse et al., 2009; Keller et al., 2011). However, other studies
87 have reported no association between HLD and structural hemispheric asymmetry in
88 classical language cortical areas (Chiarello et al. 2013; Greve et al. 2013). Attention
89 has recently shifted towards the importance of white matter as the basis of
90 lateralised cortical function. Some studies have reported that leftward language
91 lateralisation is associated with a greater volume of the arcuate fasciculus (Propper
92 et al., 2010) and the number of tracts in the corpus callosum (Timocin et al., 2020).
93 More recently, HLD has been investigated using microstructural DTI properties, such
94 as fractional anisotropy (FA), in patient cohorts (Tantillo et al., 2016; Barba et al.,

95 2020). Some studies have reported relationships between language lateralisation
96 and diffusion characteristics or the size of the corpus callosum (Tantillo et al., 2016),
97 while others did not (Barba et al., 2020). There are limited functional MRI (fMRI)-DTI
98 studies on language lateralisation in healthy individuals. Tractography studies have
99 reported associations between fMRI-determined left HLD and FA of the left arcuate
100 fasciculus (James et al., 2015; Perlaki et al., 2013; Powell et al., 2006; Silva &
101 Citterio, 2017) and corpus callosum (Häberling et al., 2011). However, other studies
102 have not reported relationships between the side or extent of HLD and conventional
103 diffusion-based tract characteristics (Karpychev et al., 2022; Vernooij et al., 2007),
104 as well as more sophisticated diffusion MRI measures, such as fibre density cross-
105 section (Verhelst et al., 2021). Inconsistencies between studies may be due to
106 methodological differences, including differences in tractography approaches, study
107 designs, patient characteristics, and sample sizes.

108 In the present study, we adopted two complementary approaches that
109 potentially overcome some of the methodological shortcomings of previous
110 tractography studies. First, we employed a connectometry approach based on an
111 local analysis of diffusion properties, which uses permutation testing to identify group
112 differences along white matter tracts. This whole-brain approach employs
113 correlational tractography to identify specific subcomponents of white matter tracts
114 that exhibit anisotropy correlated with a predefined variable of interest with superior
115 sensitivity and specificity compared to traditional voxel-based analyses (Yeh et al.,
116 2016). Connectometry has recently been used to uncover structural disparities
117 between bilingual and non-bilingual individuals (Rahmani et al., 2017) and to identify
118 structural pathways linked to enhanced language capabilities in individuals with
119 aphasia (Hula et al., 2020; Dresang et al., 2021) and preterm-born children (Barnes-
120 Davis et al., 2020, 2022). Second, we employed shape analysis to investigate the
121 geometrical characteristics of white matter tract bundles that comprise the integral
122 components of language networks. This approach captures fundamental shape
123 characteristics, such as volume and surface area, and encompasses advanced
124 morphological properties including white matter bundle curl, elongation, length, span,
125 and diameter (Yeh, 2020). Previous studies have already demonstrated, through the
126 utilization of virtual dissections (Catani et al., 2007) and shape analysis employing
127 tractography algorithms (Yeh et al., 2020), that the leftward morphometric

128 asymmetries of language-associated white matter tracts exist in people without
129 known hemispheric language dominance (HLD). Whether white matter
130 interhemispheric asymmetries change in people with atypical HLD remains unclear.

131 The first objective of the present study was to conduct diffusion
132 connectometry analysis in a large cohort of healthy individuals who underwent
133 language fMRI to determine whether microstructural properties of white matter tracts
134 are related to HLD. The second objective was to explore whether interhemispheric
135 shape asymmetries of white matter tracts are related to language lateralisation in the
136 same individuals.

137

138 **Methods**

139 *Study data and participants*

140 All data were acquired from the Human Connectome Project (HCP)
141 (<http://www.humanconnectome.org/>) open-access data initiative offering high-quality
142 anatomical and functional MRI of the human brain. We used the HCP Young Adults
143 (HCP-YA 1200 Subjects) data release as it contains a large sample of healthy adults
144 for whom both language task fMRI and diffusion MRI sequences were acquired. The
145 dataset comprised 1200 healthy adults, aged 22-35 years. Each participant
146 underwent an identical imaging protocol acquired on the same MRI scanner.
147 Individuals with neuropsychiatric or neurologic disorders, diabetes, high blood
148 pressure, premature birth, and severe symptoms associated with substance use
149 were excluded from data collection (Van Essen et al., 2013). The present study
150 focused on language fMRI and diffusion MRI data only. Individuals were only
151 selected for inclusion if they had fMRI data available for the language story task (see
152 below) and had corresponding 3T diffusion MRI data. This resulted in a sample size
153 of 1040 participants (562 females), with a mean age of 28.74 (SD = 3.69) years.
154 According to the Edinburgh Handedness Inventory (Oldfield, 1971), 962 (92%)
155 participants preferred their right hand, scoring at least 10 on a scale of -100 (left) to
156 100 (right). Eighty-five participants preferred left, scoring below -10, and two were
157 ambidextrous, scoring zero.

158

159 *Data acquisition*

160 HCP data were acquired on a Siemens 3T Skyra system, with 32-channel
161 (SC72) head coil. Task fMRI data were collected using gradient-echo echo-planar
162 imaging (EPI) with an isotropic resolution of 2.0 mm (TR = 720ms, TE = 33.1ms,
163 matrix = 104x90, 72 slices, flip angle = 52°, BW = 2290 Hz/Px, FOV = 208 x 180
164 mm, 72 slices, multiband accelerator factor = 8) (Marcus et al., 2013). The HCP
165 dMRI data were acquired using three shells (b=1000, 2000 and 3000 s/mm²) with 90
166 diffusion gradient directions and five b₀ volumes with RL phase encoding direction
167 (TE = 89.5ms, TR = 5520ms, flip angles = 78/160°, isotropic voxel size = 1.25 mm³,
168 multiband factor = 3) (Sotiropoulos et al., 2013).

169

170 *Language paradigm*

171 The language comprehension task used in Human Connectome Project was
172 designed by Binder and colleagues (2011). The task consists of two 3.8-minute runs.
173 Each run has four blocks of story tasks alternating with four blocks of math tasks.
174 The story and math tasks are matched in terms of length, word and phoneme rate,
175 speaking style, and prosodic features. The story blocks present subjects with 5-9
176 auditory sentences, followed by questions about the content of the story. The math
177 task requires participants to perform arithmetic operations followed by equals and
178 two choices. Since arithmetic tasks do not engage temporal lobe activity (Baldo &
179 Dronkers, 2007), we decided to use a STORY-MATH contrast, as it effectively
180 isolates regions responsible for language comprehension without “masking” temporal
181 lobe activity. Additionally, temporal lobe is involved in high-level processes of normal
182 consciousness (Spitsyna et al., 2006), thus we avoided passive tasks as a baseline
183 to reduce the risk of masking activities in this region (which is essential for language
184 comprehension). This contrast allowed us to cancel out the regions that are jointly
185 activated in both tasks (such as low-level auditory and phonological input), isolating
186 the regions involved in narrative processing including semantic and non-speech
187 related aspects of language, theory of mind, and inference processing.

188

189 *fMRI preprocessing and analysis*

190 The preprocessed task fMRI data were retrieved from HCP database
191 (<https://db.humanconnectome.org>). The HCP pre-processing included *fMRI/Volume*
192 and *fMRI/Surface* pipelines, which were primarily built using tools from FSL
193 (Jenkinson et al., 2012; <http://www.fmrib.ox.ac.uk/fsl>), Freesurfer (Fischl, 2012) and
194 the HCP Workbench (Marcus et al., 2013). Details of the pre-processing steps have
195 been described previously (Glasser et al., 2013). The goal of the first *fMRI/Volume*
196 pipeline was to generate 4D whole-brain timeseries. This was accomplished by (1)
197 removing spatial distortions by gradient non-linearity distortion correction, (2)
198 realigning volumes using rigid-body motion correction using a single-band reference
199 image as the target, and (3) estimating (using FSL toolbox “topup”) and correcting
200 field map-based EPI distortions. The resulting EPI data was (4) registered to T1-
201 weighted scan, then (5) non-linearly (FNIRT) into Montreal Neurological Institute
202 (MNI) space, and (6) blood-oxygen-level-dependent (BOLD) signal intensity was
203 normalized by the average. This process resulted in individual subjects being
204 mapped with a notable degree of left-right symmetry (Elam et al, 2021), which aligns
205 with laterality research recommendations (Vingerhoets et al., 2023).

206 The goal of *fMRI/Surface* pipeline was to transform the resulting 4D timeseries
207 to Connectivity Informatics Technology Initiative (CIFTI) grayordinate space,
208 encompassing cortical, subcortical, and cerebellar grey matter collectively (Pham et
209 al, 2022). This was accomplished by mapping fMRI data within cortical grey matter
210 ribbon onto the native cortical surface, registering it into CIFTI grayordinate space
211 (surface representation with 32,492 vertices on each hemisphere), and mapping the
212 set of subcortical grey matter voxels from each subcortical parcel in each individual
213 to a standard set of voxels in each atlas parcel, resulting in 2mm average surface
214 vertex and subcortical volume voxel spacing. Finally, grayordinate space data was
215 smoothed using Gaussian kernel.

216 We used a fully processed task-based STORY-MATH fMRI activation
217 Contrast Of Parameter Estimates (COPE) map, which was generated by FSL FEAT
218 and is readily available on <https://db.humanconnectome.org> as part of the “S1200
219 Subjects” dataset. Considering the spatial heterogeneity of the individual brain
220 scans, the MSM-All (Multimodal Surface Matching) registered dataset was used,
221 which uses information on areal features derived from the resting state network,
222 myelin maps, and alignment of folding. The motivation for using MSM-All over MSM-

223 Sulc (cortical folding-based registration) came from previous studies that
224 demonstrated a weaker correlation between sulcal depth and local curvature with
225 regions responsible for higher cognitive functions, including Broca's area (Fischl et
226 al., 2008; Van Essen, 2005), compared to the MSM-All registration, which showed
227 improved cross-subject alignment of independent task fMRI datasets (Robinson et
228 al., 2018).

229

230 *Language Comprehension Laterality Quotient*

231 Grayordinates localised regions-of-interest (ROIs) on the "inflated" brain
232 surface (Van Essen & Glasser, 2016). A laterality quotient (LQ) was calculated to
233 assess HLD for each participant's task fMRI activation using the CIFTI toolbox in
234 MATLAB in ROIs associated with language comprehension. The analyses were
235 conducted separately for frontal and temporal regions, given the well-documented
236 phenomenon of crossed language dominance, where a participant may exhibit
237 dominance in one hemisphere for frontal regions and the opposite hemisphere for
238 temporal regions (Seghier, 2008). For the frontal ROIs, Brodmann areas 44 and 45
239 were selected due to their established high reliability in determining language
240 dominance during semantic tasks (Sabbah et al., 2003; Seghier et al., 2008). In our
241 temporal lobe laterality analyses, ROIs were chosen within the anterior temporal lobe
242 (TGd, TGv, TE1a, TE2a, STGa, STSva, STSda) because these areas have been
243 shown to be heavily involved in language comprehension (Binder et al., 2011)
244 (Figure 1).

245 To work with CIFTI files, we generated *dscalar* files for each ROI using
246 *wb_command*, imported them into MATLAB, and extracted z-values from ROIs using
247 the CIFTI toolbox. The z-values were thresholded for each participant by including
248 only grayordinates with values greater than the median in each ROI (Dietz et al.,
249 2016). To account for the unequal number of grayordinates between the left and
250 right hemisphere (approximately 100 more grayordinates on the left than the right),
251 we corrected for these regional differences to ensure that comparisons between
252 hemispheres were not skewed by differences in their sizes. This adjustment involved
253 dividing the total sum of thresholded z-values by the number of grayordinates in
254 each hemisphere for both frontal and temporal ROIs separately. The laterality

255 quotient (LQ) was then computed for each participant's normalised z-values using
256 the equations below:

257

$$258 \quad LQ = \frac{(L - R)}{\max(L, R)}$$

259

260 Where L represents the normalised z-values in the left, and R in the right ROI.
261 We chose to employ an innovative LQ formula based on the Jaccard-Tanimoto index
262 to provide a more sophisticated approach in evaluating and classifying language
263 lateralisation (Seghier, 2019). This revised formula defines LQ as a metric of
264 distance that adheres to a consistent distribution pattern, thus enhancing its
265 sensitivity towards hemisphere activity differences, accentuating the distinctions
266 between the two hemispheres. The values above +1/3 indicate left language
267 dominance (LLD), values below -1/3 indicate right language dominance (RLD), and
268 values between -1/3 and +1/3 indicate bilateral language representation (BLR),
269 ensuring an equal cumulative probability in each dominance category.

270

271 *Diffusion processing*

272 Diffusion data was downloaded from the HCP S1200 Young Adult Data
273 Release and preprocessed using the HCP Diffusion preprocessing pipeline using
274 FMRIB diffusion toolbox in FSL. Briefly, the pipeline included b_0 image intensity
275 normalisation, removing EPI susceptibility-induced field distortions with FSL's "topup"
276 algorithm (Andersson et al, 2016), correcting for eddy current distortions, head
277 movements, and gradient nonlinearities (Glasser et al., 2013). Quality control of the
278 preprocessed diffusion MRI data was performed using DSI studio software
279 (<http://dsi-studio.labsolver.org>). An automatic quality control routine then checked the
280 b-table to ensure its accuracy (Schilling et al., 2019). The diffusion data were co-
281 registered in MNI space using q-space diffeomorphic reconstruction (Yeh & Tseng,
282 2011) to obtain the spin distribution function (SDF) with a recommended length ratio
283 of 1.25, as specified in the original study (Yeh et al., 2010) (Figure 2).

284

285 *Connectometry analysis*

286 We applied a whole-brain group connectometry analysis using DSI Studio as
287 described in previous applications (Barnes-Davis et al., 2020, 2022; Dresang et al.,
288 2021; Rahmani et al., 2017) to study the relationship between regional white matter
289 quantitative anisotropy (QA) and language lateralisation measures derived from LQs
290 (Figure 2). The connectometry approach derives the QA measure from the SDF in
291 each fibre orientation, which defines the number of anisotropic spins along that
292 direction in each streamline (Yeh et al., 2010, 2013). The anisotropy in each section
293 of a white matter tract is then correlated with the study variable (Yeh et al., 2016).
294 Unlike a voxel-based FA metric, which attributes identical anisotropy values to all
295 fibre orientations within a voxel, QA demonstrates a discerning capability by
296 identifying specific axonal orientations in each peak orientation of the SDF (Yeh et al.,
297 2013).

298 Our connectometry analyses were conducted in two phases: the initial phase
299 focused on examining the lateralisation of frontal regions during language
300 comprehension, and the subsequent phase investigated temporal regions. Initially,
301 connectometry analyses were performed on all participant groups concurrently,
302 followed by post-hoc analyses on three distinct groups separately to aid in
303 interpretation and capture varying effects related to different degrees of laterality.
304 Specifically, the first post-hoc analysis included participants with LLD and BLR, the
305 second consisted of participants with RLD and BLR, and the third included
306 individuals with both LLD and RLD. The linear effect of handedness, sex, and age
307 was mitigated using a partial linear correlation. A nonparametric Spearman partial
308 correlation was used to derive the continuous segments correlating with a LQ (Yeh
309 et al., 2016). Each reconstructed white matter tract within a voxel was tracked to
310 extract a QA map for each participant (Yeh et al., 2013). A T-score threshold was
311 assigned to the highest level of three to reduce the possibility of false positive results
312 (Ashraf-Ganjouei et al., 2019). The tracks were filtered by topology-informed pruning
313 with sixteen iterations to remove implausible spurious connections (Yeh et al., 2019).
314 Given the large sample size in our study, and to prevent false positives, a
315 conservative false discovery rate (FDR) correction for multiple comparisons was

316 employed with a threshold of 0.01 to select tracks showing significant associations
317 between LQ and QA. To estimate the false discovery rate, 5000 randomized
318 permutations were applied to the group label to obtain the null distribution of the
319 track length. After the correlational results were obtained, additional categorical
320 analyses were performed at the group level (LLD/RLD, LLD/BLR, RLD/BLR). Short
321 tracts (<20mm) were removed for easier interpretation of our results.

322

323 Shape analysis

324 The SDF maps generated from the connectometry analysis were used for
325 tract shape analysis and automatic fibre tractography was performed using a
326 deterministic fibre tracking algorithm utilising DSI studio software (Yeh, 2020).
327 Eleven white matter tract bundles that are part of language comprehension networks
328 (Friederici et al., 2007; Harvey et al., 2013; Ivanova et al., 2021; Rollans & Cummine,
329 2018; Shin et al., 2019; Zhong et al., 2022; Forkel et al, 2022) were then
330 automatically tracked and recognised based on the HCP-842 tractography atlas (Yeh
331 et al., 2018) (Figure 3). These include the arcuate fasciculus (AF), corpus callosum
332 body, corpus callosum forceps major (splenium), corpus callosum forceps minor
333 (genu), inferior fronto-occipital fasciculus (IFOF), frontal aslant tract (FAT), inferior
334 longitudinal fasciculus (ILF), the three branches of the superior longitudinal
335 fasciculus (dorsal SLF1, middle SLF2 and ventral SLF3), and the uncinate
336 fasciculus. All white matter bundles were independently tracked within the left and
337 right hemispheres, while the corpus callosum bundles were tracked as a whole. The
338 diffusion sampling length ratio was set at 1.25 and the output resolution was
339 resampled to 2 mm isotropic. To remove false connections, topology-informed
340 pruning was applied with 32 iterations (Yeh et al., 2019). We decided to exclude
341 participants for whom we could not reconstruct at least one of their ROI bundles. As
342 a result, 290 participants were excluded, leaving us with a final sample size of 750
343 participants. Finally, after identifying all white matter tracts of interest, the following
344 shape metrics were extracted: tract length, span, curl, elongation, diameter, volume,
345 and surface area were extracted (Figure 4).

346 To evaluate the statistical significance of differences among various laterality
347 groups (LLD, RLD, BLR), we conducted an analysis of variance (ANOVA). This

348 analysis utilized the same laterality groupings based on frontal and temporal ROIs
349 and included covariates consistent with those used in the connectometry analyses.
350 All computations were performed using R (version 4.4.1).

351

352 **Results**

353 *fMRI*

354 Activations in frontal ROIs revealed a weak leftward lateralisation on the
355 group level ($LQ=0.33\pm 0.31$), while BOLD activations in anterior temporal lobe ROIs
356 showed a more bilateral pattern ($LQ=0.17\pm 0.2$). Based on the frontal ROIs of the
357 fMRI language comprehension task, 581 participants were classified as left-
358 hemisphere dominant (56%; $LQ=0.53\pm 0.16$), 426 as bilateral (41%; $LQ=0.13\pm 0.17$),
359 and the remaining 33 as right-hemisphere dominant (3%; $LQ=-0.64\pm 0.17$). For
360 temporal ROIs, only 193 participants (19%; $LQ=0.41\pm 0.09$) were left-hemisphere
361 dominant, while 80% ($n=833$) were classified as bilateral ($LQ=0.13\pm 0.14$). Only 14
362 participants (1%; $LQ=-0.58\pm 0.28$) were right lateralised. In both laterality groups,
363 strong neural activity is observed in brain areas associated with semantic processing
364 i.e. anterior, and posterior temporal lobes as well as in the left inferior frontal gyrus
365 (Jackson, 2021) (Figure 5). In line with previous reports that have used similar
366 story/narrative materials, also the ventral angular gyrus bordering the
367 temporoparietal junction was engaged during language comprehension (Lerner et al,
368 2011; Branzi et al, 2020; Branzi et al., 2021; Humbphreys & Lambon Ralph, 2015).

369

370 *Connectometry*

371 Two connectometry analyses were conducted. Firstly, in the investigation of
372 language lateralisation in frontal regions, a total of 2028 white matter tracts exhibiting
373 a significant negative correlation with LQ ($n=1040$; $p<0.01$, FDR corrected) were
374 identified. Notably, the majority of these tracts were commissural, constituting 82% of
375 the identified tracts, including the forceps minor (63%) and corpus callosum body
376 (19%). A smaller portion of these tracts were positioned in bilateral fornix (18%).
377 Conversely, 218 tracts were linked to higher frontal LQ values, all of which were
378 situated in bilateral cingulum ($n=1040$; $p<0.01$, FDR corrected). Subsequently,

379 categorical post-hoc analyses were conducted to further illustrate the laterality
380 groups influencing significant differences, with a specific focus on the disparities
381 between LLD and BLR, RLD and BLR, and RLD and LLD. Within the cohort of
382 bilateral and left lateralised individuals (n=1007), it was observed that individuals with
383 left lateralisation exhibited higher QA in 2126 tracts, predominantly in the forceps
384 minor (48%), corpus callosum body (38%), and bilateral fornix (8%), implying that the
385 negative correlations in the primary findings were mainly driven by individuals with
386 bilateral language dominance ($p < 0.01$, FDR corrected). The remaining streamlines
387 consisted of the right IFOF, right AF, and middle cerebellar peduncle (MCP). No
388 tracts were found to be associated with left lateralised individuals. In the analysis
389 encompassing individuals with bilateral and right hemisphere dominance (n=459),
390 only 20 streamlines in the forceps minor exhibited higher QA in individuals with right
391 hemisphere dominance compared to those with bilateral dominance ($p < 0.01$, FDR
392 corrected). No significant differences were observed between LLD and RLD (n =
393 614; $p < 0.01$, FDR corrected).

394 The second connectometry analysis revealed a significantly negative
395 correlation between anterior temporal lobe LQ and QA in 2,408 tracts (n=1040;
396 $p < 0.01$, FDR corrected). These tracts were predominantly located in the corpus
397 callosum body (67%), with additional distributions in the left corticospinal tract (9%),
398 left cingulum (7%), left medial lemniscus (5%), right dentarubrothalamic tract (3%),
399 and bilateral AF (3%). Additionally, 118 tracts showed a positive correlation between
400 QA and higher LQ in the anterior temporal regions, all of which were located in the
401 forceps minor (n=1040; $p < 0.01$, FDR corrected). Categorical post-hoc analyses
402 found no significant differences between LLD and BLR (n=1029; $p < 0.01$, FDR
403 corrected) or between RLD and BLR (n=847; $p < 0.01$, FDR corrected). However, LLD
404 and RLD comparison (n=210) identified 391 streamlines with higher QA in RLD
405 compared to LLD. These streamlines were distributed in the forceps minor (29%),
406 corpus callosum tapetum (27%), bilateral arcuate fasciculus (26%), and right IFOF
407 (8%).

408

409 *Shape analysis*

410 ANOVA analysis for language lateralisation in anterior temporal lobe showed
411 that mean length of right IFOF was significantly different between three laterality
412 groups ($F_2 = 9.8$; $p = 0.005$, FDR corrected). Tukey post-hoc tests showed that left
413 lateralised individuals had longer right IFOF compared to people with BLR ($p = 0.01$,
414 FWE corrected). Another tract that showed significant difference was forceps minor,
415 with different mean lengths between laterality groups ($F_2 = 10.1$; $p = 0.005$, FDR
416 corrected). Similarly, Tukey post-hoc tests showed that left lateralised people had
417 longer forceps minor compared to bilateral individuals ($p = 0.01$, FWE corrected)
418 (Figure 7). No significant differences between frontal laterality groups were found in
419 relation to shape metrics.

420

421 Discussion

422 *Biological implications*

423 We report significantly increased QA of the corpus callosum in individuals who
424 had lower LQ in both frontal and temporal ROIs. Post-hoc analyses revealed that this
425 result was driven by individuals with both BLR and RLD when laterality quotient was
426 calculated using frontal regions, and by RLD when laterality quotient was based on
427 the anterior temporal lobe. This observation aligns with prior research in patient
428 cohorts (Tantillo et al., 2016) and supports the hypothesis that individuals who rely
429 more on both cerebral hemispheres for language processing may have more
430 developed commissural fibres. These fibres could potentially serve as a
431 compensatory mechanism for the heightened metabolic energy requirements
432 associated with information transfer and the reduction of transmission times
433 (Laughlin & Sejnowski, 2003). An alternative hypothesis suggests that using both
434 hemispheres for language processing is more natural than previously thought
435 (Newport et al., 2022). This implies that the shift of language function towards the left
436 hemisphere might result from less developed commissural tracts. Well-developed
437 commissural tracts may facilitate bilateral language processing in frontal regions by
438 allowing the right hemisphere to participate fully in language tasks (Newport et al.,
439 2017). A higher forceps minor anisotropy in right lateralised people compared to
440 people with LLD and BLR (Figures 6-1, 7-1) suggests that commissural tracts may

441 not necessarily enhance the function of both hemispheres but rather maintain right
442 hemisphere involvement in language comprehension tasks.

443 Other imaging research has also suggested the importance of the corpus
444 callosum for language lateralisation, although the link between structural measures
445 of the corpus callosum and HLD is unclear. One study reported a greater FA of the
446 whole corpus callosum in people with atypical language lateralisation (defined as
447 RLD and BLR together) and, consistent with our results of anterior temporal lobe
448 lateralisation, greatest anisotropy in people with RLD (Häberling et al., 2011). We
449 found a positive correlation between a small segment of the left forceps minor and
450 temporal LQ, suggesting a more complex role of the forceps minor than previously
451 understood (Figure 6). This finding was supported by shape analysis, which revealed
452 a longer forceps minor in individuals with left temporal language lateralisation. This
453 aligns with a recent study using fixel-based analysis, which reported greater left fibre
454 bundle cross-section asymmetry of the forceps minor in individuals with left language
455 dominance (LLD) and higher asymmetry of the right forceps minor in those with RLD
456 (Verhelst et al., 2021). Thus, while the body of the corpus callosum is associated
457 with atypical (both bilateral and right) lateralisation for language comprehension in
458 our study, the posterior and anterior parts of the corpus callosum are mainly
459 associated with lateralised language, whether right or left, consistent with previous
460 studies (Karpychev et al., 2022; Westerhausen et al., 2006). Although commissural
461 fibres have shown relationships with language lateralisation in both previous and
462 current studies, there is inconsistency regarding which individuals exhibit greater
463 microstructural differences inferred by diffusion scalar metrics. This inconsistency
464 may stem from methodological factors, such as the inclusion or exclusion of
465 individuals with BLR and the type of language lateralisation assessed.

466 Our study reported a significant association between asymmetry in frontal
467 activation and QA in the fornix bilaterally, particularly in individuals exhibiting an LQ
468 closer to zero, indicating a more bilateral hemispheric representation. While there is
469 limited existing literature on the relationship between HLD and diffusion measures in
470 these tracts, some have highlighted the involvement of them in language processing
471 (Hula et al., 2020; Sihvonen et al., 2021). Our findings related to temporal lobe
472 laterality revealed a small number of streamlines in the AF bilaterally exhibiting
473 higher anisotropy in individuals with RLD compared to LLD, but not in those with

474 BLR compared to LLD. This suggests that increased QA in these regions may be
475 linked to right-hemisphere language lateralisation. Previous research has also found
476 associations between AF asymmetry and language lateralisation in several cohorts
477 of healthy individuals (Ocklenburg et al., 2013; Propper et al., 2010), although the
478 exact relationship between AF asymmetry and HLD remains unclear (Gerrits et al.,
479 2022; Verhelst et al., 2021). Further studies are needed to better understand these
480 tracts' importance for language lateralisation.

481

482 *Methodological considerations*

483 To investigate the relationship between language lateralisation and white
484 matter characteristics, we used both correlational methods and traditional categorical
485 classifications (left, right, bilateral). Analysing raw LQ values for the entire sample
486 helped reduce the subjectivity inherent in categorical groupings (Wegrzyn et al.,
487 2019; Westerhausen et al., 2006). Instead of relying solely on global BOLD
488 activation patterns to assess language lateralisation, we conducted two distinct
489 studies focusing on the frontal and anterior temporal lobes. This approach allowed
490 us to obtain more detailed insights. For instance, whilst lower LQs in both frontal and
491 temporal regions were associated with increased anisotropy in the corpus callosum,
492 frontal regions engaged a larger portion of the anterior corpus callosum body and the
493 forceps minor. Interestingly, lower LQs in the temporal lobe were linked to increased
494 anisotropy in the bilateral AF, which suggested a right hemisphere dominance, as
495 indicated by post-hoc analyses—an effect not observed in the frontal lobe.
496 Furthermore, while frontal LQs were positively correlated with fractional anisotropy in
497 the bilateral cingulum, temporal LQs were associated with increased QA in the left
498 forceps minor. Analysing language lateralisation separately for the frontal and
499 temporal regions thus provided richer and more nuanced insights into the
500 relationship between language comprehension and white matter characteristics.

501 The number of individuals with right hemisphere dominance, especially for
502 anterior temporal region, is small in the present study compared to previous studies
503 (Chang et al., 2011). This disparity is primarily attributed to the task used to assess
504 HLD, which entailed semantic processing, resulting in more bilateral fMRI activations
505 (Binder et al., 2011; Metoki et al., 2022; Walenski et al., 2019). This might be

506 because comprehension tasks rely less on the left-lateralised dorsal pathway,
507 strongly associated with cognitive operations crucial for language production (e.g.,
508 retrieval and production of speech sounds) (Hickok & Poeppel 2007). Other non-
509 mutually exclusive explanations include differences in the complexity of the linguistic
510 stimuli (single words typically used in fluency tasks versus sentences typically used
511 in comprehension tasks) and the demands that these tasks typically involve (see
512 Peelle, 2012). For example, the verbal stimuli used for the stories likely portray
513 social concepts (e.g., theory of mind, intention, emotion, morality) and/or they may
514 contain different amounts of metaphor, idiom, or implied meaning. All these aspects
515 have been associated with the recruitment of fronto-temporal and parietal regions in
516 the right hemisphere (Miller et al. 1997; Olson et al. 2007; Yang, 2014; Schmidt et
517 al., 2007).

518 The fact that we employed a language comprehension task might explain why
519 only a small subset of participants demonstrated strong leftward lateralisation, while
520 the majority displayed mild lateralisation. A recent systematic review comparing
521 different language tasks has highlighted that language production tasks may be
522 more robust in accurately assessing language laterality than language
523 comprehension tasks (Bradshaw et al., 2017). For instance, there is evidence that
524 between 6 and 24 years of age, there is an increase in frontal asymmetry during
525 tasks involving the articulation of words. However, this asymmetry is not present
526 during story listening. This suggests partly different maturational mechanisms
527 between language comprehension and production (Lidzba et al., 2011; Berl et al.,
528 2010). Future studies will have to use tasks that typically generate strongly left
529 lateralised neural responses such as verbal fluency tasks to corroborate our findings.

530 Our methodology offers several practical benefits. Firstly, despite the limited
531 proportion of right hemisphere dominant individuals identified through the functional
532 language task, the sizeable sample size (N= 1040) employed in this study is the
533 largest ever utilised in such investigations, thus potentially decreasing the likelihood
534 of false positives. Secondly, we employed two complementary methodologies,
535 namely connectometry and tractography, to delineate the precise white matter
536 characteristics associated with HLD. In doing so, we have provided new insights into
537 the anatomical basis of language lateralisation insomuch that white matter tract
538 geometrical features (shape analysis) are unrelated to HLD at the group-level.

539

540 **Conclusion**

541 The findings of our study suggest that measures of diffusion-based
542 microstructural architecture of reconstructed white matter tracts, are linked to
543 language lateralisation. Specifically, individuals who exhibit a greater reliance on
544 both cerebral hemispheres for language comprehension may possess more highly
545 developed CC body fibres, thereby promoting more efficient interhemispheric
546 communication. The involvement of anterior and posterior parts of the CC in
547 asymmetrical temporal lobe activity (i.e., either left or right) for language
548 comprehension unveils a more complex and nuanced role of the forceps minor.
549 Future research should further investigate these relationships, employing tasks that
550 typically generate strongly left-lateralized neural responses, to validate and expand
551 upon our findings.

552

553 **References**

- 554 Andersson, J. L., & Sotiropoulos, S. N. (2016). An integrated approach to correction
555 for off-resonance effects and subject movement in diffusion MR imaging.
556 *Neuroimage*, 125, 1063-1078.
- 557
- 558 Ashraf-Ganjouei, A., Rahmani, F., Aarabi, M. H., Sanjari Moghaddam, H., Nazem-
559 Zadeh, M. R., Davoodi-Bojd, E., & Soltanian-Zadeh, H. (2019). White matter
560 correlates of disease duration in patients with temporal lobe epilepsy: updated
561 review of literature. *Neurological Sciences*, 40, 1209-1216.
- 562
- 563 Baldo, J. V., & Dronkers, N. F. (2007). Neural correlates of arithmetic and language
564 comprehension: A common substrate?. *Neuropsychologia*, 45(2), 229-235.
- 565
- 566 Barba, C., Montanaro, D., Grisotto, L., Frijia, F., Pellacani, S., Cavalli, A., ... &
567 Guerrini, R. (2020). Patterns and predictors of language representation and the
568 influence of epilepsy surgery on language reorganization in children and young
569 adults with focal lesional epilepsy. *Plos one*, 15(9), e0238389.
- 570
- 571 Barnes-Davis, M. E., Williamson, B. J., Merhar, S. L., Holland, S. K., & Kadis, D. S.
572 (2020). Extremely preterm children exhibit altered cortical thickness in language
573 areas. *Scientific reports*, 10(1), 10824.
- 574

- 575 Barnes-Davis, M. E., Williamson, B. J., Merhar, S. L., Nagaraj, U. D., Parikh, N. A., &
576 Kadis, D. S. (2022). Extracallosal structural connectivity is positively associated with
577 language performance in well-performing children born extremely preterm. *Frontiers*
578 *in Pediatrics*, 10, 821121.
- 579
- 580 Berl, M. M., Duke, E. S., Mayo, J., Rosenberger, L. R., Moore, E. N., VanMeter, J., ...
581 & Gaillard, W. D. (2010). Functional anatomy of listening and reading
582 comprehension during development. *Brain and language*, 114(2), 115-125.
- 583
- 584 Binder, J. R., Gross, W. L., Allendorfer, J. B., Bonilha, L., Chapin, J., Edwards, J. C.,
585 ... & Weaver, K. E. (2011). Mapping anterior temporal lobe language areas with
586 fMRI: a multicenter normative study. *Neuroimage*, 54(2), 1465-1475.
- 587
- 588 Bradshaw, A. R., Thompson, P. A., Wilson, A. C., Bishop, D. V., & Woodhead, Z. V.
589 (2017). Measuring language lateralisation with different language tasks: a systematic
590 review. *PeerJ*, 5, e3929.
- 591
- 592 Branzi, F. M., Humphreys, G. F., Hoffman, P., & Ralph, M. A. L. (2020). Revealing
593 the neural networks that extract conceptual gestalts from continuously evolving or
594 changing semantic contexts. *NeuroImage*, 220, 116802.
- 595
- 596 Branzi, F. M., Pobric, G., Jung, J., & Lambon Ralph, M. A. (2021). The left angular
597 gyrus is causally involved in context-dependent integration and associative encoding
598 during narrative reading. *Journal of cognitive neuroscience*, 33(6), 1082-1095.
- 599
- 600 Catani, M., Allin, M. P., Husain, M., Pugliese, L., Mesulam, M. M., Murray, R. M., &
601 Jones, D. K. (2007). Symmetries in human brain language pathways correlate with
602 verbal recall. *Proceedings of the National Academy of Sciences*, 104(43), 17163-
603 17168.
- 604
- 605 Chang, E. F., Wang, D. D., Perry, D. W., Barbaro, N. M., & Berger, M. S. (2011).
606 Homotopic organization of essential language sites in right and bilateral cerebral
607 hemispheric dominance. *Journal of neurosurgery*, 114(4), 893-902.
- 608
- 609 Chiarello, C., Vazquez, D., Felton, A., & Leonard, C. M. (2013). Structural
610 asymmetry of anterior insula: Behavioral correlates and individual differences. *Brain*
611 *and language*, 126(2), 109-122.
- 612
- 613 De Schotten, M. T., Bizzi, A., Dell'Acqua, F., Allin, M., Walshe, M., Murray, R., ... &
614 Catani, M. (2011). Atlasing location, asymmetry and inter-subject variability of white
615 matter tracts in the human brain with MR diffusion tractography. *Neuroimage*, 54(1),
616 49-59.
- 617

- 618 Dietz, A., Vannest, J., Maloney, T., Altaye, M., Szaflarski, J. P., & Holland, S. K.
619 (2016). The calculation of language lateralization indices in post-stroke aphasia: A
620 comparison of a standard and a lesion-adjusted formula. *Frontiers in Human*
621 *Neuroscience*, 10, 493.
- 622
- 623 Dorsaint-Pierre, R., Penhune, V. B., Watkins, K. E., Neelin, P., Lerch, J. P., Bouffard,
624 M., & Zatorre, R. J. (2006). Asymmetries of the planum temporale and Heschl's
625 gyrus: relationship to language lateralisation. *Brain*, 129(5), 1164-1176.
- 626
- 627 Dresang, H. C., Hula, W. D., Yeh, F. C., Warren, T., & Dickey, M. W. (2021). White-
628 matter neuroanatomical predictors of aphasic verb retrieval. *Brain*
629 *Connectivity*, 11(4), 319-330.
- 630
- 631 Elam, J. S., Glasser, M. F., Harms, M. P., Sotiropoulos, S. N., Andersson, J. L.,
632 Burgess, G. C., ... & Van Essen, D. C. (2021). The human connectome project: a
633 retrospective. *NeuroImage*, 244, 118543.
- 634
- 635 Fischl, B., Rajendran, N., Busa, E., Augustinack, J., Hinds, O., Yeo, B. T., ... & Zilles,
636 K. (2008). Cortical folding patterns and predicting cytoarchitecture. *Cerebral*
637 *cortex*, 18(8), 1973-1980.
- 638
- 639 Fischl, B. (2012). FreeSurfer. *Neuroimage*, 62(2), 774-781.
- 640
- 641 Forkel, S. J., Friedrich, P., Thiebaut de Schotten, M., & Howells, H. (2022). White
642 matter variability, cognition, and disorders: a systematic review. *Brain Structure and*
643 *Function*, 1-16.
- 644
- 645 Foundas, A. L., Leonard, C. M., Gilmore, R. L., Fennell, E. B., & Heilman, K. M.
646 (1996). Pars triangularis asymmetry and language dominance. *Proceedings of the*
647 *National Academy of Sciences*, 93(2), 719-722.
- 648
- 649 Friederici, A. D., von Cramon, D. Y., & Kotz, S. A. (2007). Role of the corpus
650 callosum in speech comprehension: interfacing syntax and prosody. *Neuron*, 53(1),
651 135-145.
- 652
- 653 Gerrits, R., Verhelst, H., Dhollander, T., Xiang, L., & Vingerhoets, G. (2022).
654 Structural perisylvian asymmetry in naturally occurring atypical language
655 dominance. *Brain Structure and Function*, 227(2), 573-586.
- 656
- 657 Glasser, M. F., Sotiropoulos, S. N., Wilson, J. A., Coalson, T. S., Fischl, B.,
658 Andersson, J. L., ... & Wu-Minn HCP Consortium. (2013). The minimal
659 preprocessing pipelines for the Human Connectome Project. *Neuroimage*, 80, 105-
660 124.
- 661

- 662 Glasser, M. F., Coalson, T. S., Robinson, E. C., Hacker, C. D., Harwell, J., Yacoub,
663 E., ... & Van Essen, D. C. (2016). A multi-modal parcellation of human cerebral
664 cortex. *Nature*, 536(7615), 171-178.
665
- 666 Greve, D. N., Van der Haegen, L., Cai, Q., Stufflebeam, S., Sabuncu, M. R., Fischl,
667 B., & Brysbaert, M. (2013). A surface-based analysis of language lateralisation and
668 cortical asymmetry. *Journal of cognitive neuroscience*, 25(9), 1477-1492.
669
- 670 Güntürkün, O., Ströckens, F., & Ocklenburg, S. (2020). Brain lateralization: a
671 comparative perspective. *Physiological reviews*.
672
- 673 Häberling, I. S., Badzakova-Trajkov, G., & Corballis, M. C. (2011). Callosal tracts
674 and patterns of hemispheric dominance: a combined fMRI and DTI
675 study. *Neuroimage*, 54(2), 779-786.
676
- 677 Harvey, D. Y., Wei, T., Ellmore, T. M., Hamilton, A. C., & Schnur, T. T. (2013).
678 Neuropsychological evidence for the functional role of the uncinate fasciculus in
679 semantic control. *Neuropsychologia*, 51(5), 789-801.
680
- 681 Hickok, G., & Poeppel, D. (2007). The cortical organization of speech processing.
682 *Nature reviews neuroscience*, 8(5), 393-402.
683
- 684 Hula, W. D., Panesar, S., Gravier, M. L., Yeh, F. C., Dresang, H. C., Dickey, M. W.,
685 & Fernandez-Miranda, J. C. (2020). Structural white matter connectometry of word
686 production in aphasia: an observational study. *Brain*, 143(8), 2532-2544.
687
- 688 Ivanova, M. V., Zhong, A., Turken, A., Baldo, J. V., & Dronkers, N. F. (2021).
689 Functional contributions of the arcuate fasciculus to language processing. *Frontiers*
690 *in human neuroscience*, 15, 672665.
691
- 692 Jackson, R. L. (2021). The neural correlates of semantic control revisited.
693 *NeuroImage*, 224, 117444.
694
- 695 James, J. S., Kumari, S. R., Sreedharan, R. M., Thomas, B., Radhkrishnan, A., &
696 Kesavadas, C. (2015). Analyzing functional, structural, and anatomical correlation of
697 hemispheric language lateralisation in healthy subjects using functional MRI,
698 diffusion tensor imaging, and voxel-based morphometry. *Neurology India*, 63(1), 49.
699
- 700 Jenkinson, M., Beckmann, C. F., Behrens, T. E., Woolrich, M. W., & Smith, S. M.
701 (2012). Fsl. *Neuroimage*, 62(2), 782-790.
702
- 703 Josse, G., Kherif, F., Flandin, G., Seghier, M. L., & Price, C. J. (2009). Predicting
704 language lateralisation from gray matter. *Journal of Neuroscience*, 29(43), 13516-
705 13523.

- 706
707 Karpychev, V., Bolgina, T., Malytina, S., Zinchenko, V., Ushakov, V., Ignatyev, G., &
708 Dragoy, O. (2022). Greater volumes of a callosal sub-region terminating in posterior
709 language-related areas predict a stronger degree of language lateralisation: A
710 tractography study. *Plos one*, 17(12), e0276721.
- 711
712 Keller, S. S., Roberts, N., García-Fiñana, M., Mohammadi, S., Ringelstein, E. B.,
713 Knecht, S., & Deppe, M. (2011). Can the language-dominant hemisphere be
714 predicted by brain anatomy?. *Journal of Cognitive Neuroscience*, 23(8), 2013-2029.
- 715
716 Keller, S. S., Roberts, N., Baker, G., Sluming, V., Cezayirli, E., Mayes, A., ... &
717 Wiesmann, U. C. (2018). A voxel-based asymmetry study of the relationship
718 between hemispheric asymmetry and language dominance in Wada tested
719 patients. *Human brain mapping*, 39(7), 3032-3045.
- 720
721 Laughlin, S. B., & Sejnowski, T. J. (2003). Communication in neuronal
722 networks. *Science*, 301(5641), 1870-1874.
- 723
724 Lerner, Y., Honey, C. J., Silbert, L. J., & Hasson, U. (2011). Topographic mapping of
725 a hierarchy of temporal receptive windows using a narrated story. *Journal of*
726 *Neuroscience*, 31(8), 2906-2915.
- 727
728 Lidzba, K., Schwilling, E., Grodd, W., Krägeloh-Mann, I., & Wilke, M. (2011).
729 Language comprehension vs. language production: age effects on fMRI activation.
730 *Brain and language*, 119(1), 6-15.
- 731
732 Marcus, D. S., Harms, M. P., Snyder, A. Z., Jenkinson, M., Wilson, J. A., Glasser, M.
733 F., ... & WU-Minn HCP Consortium. (2013). Human Connectome Project informatics:
734 quality control, database services, and data visualization. *Neuroimage*, 80, 202-219.
- 735
736 Metoki, A., Wang, Y., & Olson, I. R. (2022). The social cerebellum: a large-scale
737 investigation of functional and structural specificity and connectivity. *Cerebral*
738 *Cortex*, 32(5), 987-1003.
- 739
740 Newport, E. L., Seydell-Greenwald, A., Landau, B., Turkeltaub, P. E., Chambers, C.
741 E., Martin, K. C., ... & Gaillard, W. D. (2022). Language and developmental plasticity
742 after perinatal stroke. *Proceedings of the National Academy of Sciences*, 119(42),
743 e2207293119.
- 744
745 Newport, E. L., Landau, B., Seydell-Greenwald, A., Turkeltaub, P. E., Chambers, C.
746 E., Dromerick, A. W., ... & Gaillard, W. D. (2017). Revisiting Lenneberg's hypotheses
747 about early developmental plasticity: Language organization after left-hemisphere
748 perinatal stroke. *Biolinguistics*, 11, 407.
- 749

- 750 Ocklenburg, S., Hugdahl, K., & Westerhausen, R. (2013). Structural white matter
751 asymmetries in relation to functional asymmetries during speech perception and
752 production. *Neuroimage*, 83, 1088-1097.
753
- 754 Oldfield, R. C. (1971). The assessment and analysis of handedness: the Edinburgh
755 inventory. *Neuropsychologia*, 9(1), 97-113.
756
- 757 Peelle, J. E. (2012). The hemispheric lateralization of speech processing depends on
758 what "speech" is: a hierarchical perspective. *Frontiers in human neuroscience*, 6,
759 309.
760
- 761 Perlaki, G., Horvath, R., Orsi, G., Aradi, M., Auer, T., Varga, E., ... & Janszky, J.
762 (2013). White-matter microstructure and language lateralisation in left-handers: a
763 whole-brain MRI analysis. *Brain and Cognition*, 82(3), 319-328.
764
- 765 Pham, D. D., Muschelli, J., & Mejia, A. F. (2022). ciftiTools: A package for reading,
766 writing, visualizing, and manipulating CIFTI files in R. *NeuroImage*, 250, 118877.
767
- 768 Powell, H. R., Parker, G. J., Alexander, D. C., Symms, M. R., Boulby, P. A.,
769 Wheeler-Kingshott, C. A., ... & Duncan, J. S. (2006). Hemispheric asymmetries in
770 language-related pathways: a combined functional MRI and tractography
771 study. *Neuroimage*, 32(1), 388-399.
772
- 773 Propper, R. E., O'Donnell, L. J., Whalen, S., Tie, Y., Norton, I. H., Suarez, R. O., ... &
774 Golby, A. J. (2010). A combined fMRI and DTI examination of functional language
775 lateralisation and arcuate fasciculus structure: Effects of degree versus direction of
776 hand preference. *Brain and cognition*, 73(2), 85-92.
777
- 778 Rahmani, F., Sobhani, S., & Aarabi, M. H. (2017). Sequential language learning and
779 language immersion in bilingualism: diffusion MRI connectometry reveals
780 microstructural evidence. *Experimental brain research*, 235(10), 2935-2945.
781
- 782 Robinson, E. C., Garcia, K., Glasser, M. F., Chen, Z., Coalson, T. S., Makropoulos,
783 A., ... & Rueckert, D. (2018). Multimodal surface matching with higher-order
784 smoothness constraints. *Neuroimage*, 167, 453-465.
785
- 786 Rodrigo, S., Oppenheim, C., Chassoux, F., Hodel, J., De Vanssay, A., Baudoin-
787 Chial, S., ... & Meder, J. F. (2008). Language lateralisation in temporal lobe epilepsy
788 using functional MRI and probabilistic tractography. *Epilepsia*, 49(8), 1367-1376.
789
- 790 Rollans, C., & Cummine, J. (2018). One tract, two tract, old tract, new tract: A pilot
791 study of the structural and functional differentiation of the inferior fronto-occipital
792 fasciculus. *Journal of Neurolinguistics*, 46, 122-137.
793

- 794 Sabbah, P., Chassoux, F., Leveque, C., Landre, E., Baudoin-Chial, S., Devaux, B.,
795 ... & Cordoliani, Y. S. (2003). Functional MR imaging in assessment of language
796 dominance in epileptic patients. *Neuroimage*, 18(2), 460-467.
797
- 798 Schilling, K. G., Yeh, F. C., Nath, V., Hansen, C., Williams, O., Resnick, S., ... &
799 Landman, B. A. (2019). A fiber coherence index for quality control of B-table
800 orientation in diffusion MRI scans. *Magnetic resonance imaging*, 58, 82-89.
801
- 802 Seghier, M. L. (2008). Laterality index in functional MRI: methodological issues.
803 *Magnetic resonance imaging*, 26(5), 594-601.
804
- 805 Seghier, M. L., Lazeyras, F., Pegna, A. J., Annoni, J. M., & Khateb, A. (2008). Group
806 analysis and the subject factor in functional magnetic resonance imaging: Analysis of
807 fifty right-handed healthy subjects in a semantic language task. *Human brain*
808 *mapping*, 29(4), 461-477.
809
- 810 Seghier, M. L. (2019). Categorical laterality indices in fMRI: a parallel with classic
811 similarity indices. *Brain Structure and Function*, 224, 1377-1383.
812
- 813 Shin, J., Rowley, J., Chowdhury, R., Jolicoeur, P., Klein, D., Grova, C., ... &
814 Kobayashi, E. (2019). Inferior longitudinal fasciculus' role in visual processing and
815 language comprehension: a combined MEG-DTI study. *Frontiers in*
816 *Neuroscience*, 13, 875.
817
- 818 Sihvonen, A. J., Virtala, P., Thiede, A., Laasonen, M., & Kujala, T. (2021). Structural
819 white matter connectometry of reading and dyslexia. *NeuroImage*, 241, 118411.
820
- 821 Silva, G., & Citterio, A. (2017). Hemispheric asymmetries in dorsal language
822 pathway white-matter tracts: a magnetic resonance imaging tractography and
823 functional magnetic resonance imaging study. *The Neuroradiology Journal*, 30(5),
824 470-476.
825
- 826 Sotiropoulos, S. N., Jbabdi, S., Xu, J., Andersson, J. L., Moeller, S., Auerbach, E. J.,
827 ... & Wu-Minn Hcp Consortium. (2013). Advances in diffusion MRI acquisition and
828 processing in the Human Connectome Project. *Neuroimage*, 80, 125-143.
829
- 830 Spitsyna, G., Warren, J. E., Scott, S. K., Turkheimer, F. E., & Wise, R. J. (2006).
831 Converging language streams in the human temporal lobe. *Journal of Neuroscience*,
832 26(28), 7328-7336.
833
- 834 Tantillo, G., Peck, K. K., Arevalo-Perez, J., Lyo, J. K., Chou, J. F., Young, R. J., ... &
835 Holodny, A. I. (2016). Corpus callosum diffusion and language lateralisation in
836 patients with brain tumors: a DTI and fMRI study. *Journal of Neuroimaging*, 26(2),
837 224-231.

- 838
839 Timocin, G., Toprak, A., & Aralasmak, A. (2020). Relationships of language
840 lateralisation with diffusion tensor imaging metrics of corpus callosum, tumor grade,
841 and tumors distance to language-eloquent areas in glial neoplasms. *Journal of*
842 *Computer Assisted Tomography*, 44(6), 956-968.
- 843
844 Van Essen, D. C. (2005). A population-average, landmark-and surface-based
845 (PALS) atlas of human cerebral cortex. *Neuroimage*, 28(3), 635-662.
- 846
847 Van Essen, D. C., Smith, S. M., Barch, D. M., Behrens, T. E., Yacoub, E., Ugurbil,
848 K., & Wu-Minn HCP Consortium. (2013). The WU-Minn human connectome project:
849 an overview. *Neuroimage*, 80, 62-79.
- 850
851 Van Essen, D. C., & Glasser, M. F. (2016). The human connectome project:
852 Progress and prospects. In *Cerebrum: the Dana forum on brain science* (Vol. 2016).
853 Dana Foundation.
- 854
855 Vias, C., & Dick, A. S. (2017). Cerebellar contributions to language in typical and
856 atypical development: a review. *Developmental neuropsychology*, 42(6), 404-421.
- 857
858 Verhelst, H., Dhollander, T., Gerrits, R., & Vingerhoets, G. (2021). Fibre-specific
859 laterality of white matter in left and right language dominant
860 people. *NeuroImage*, 230, 117812.
- 861
862 Vernooij, M. W., Smits, M., Wielopolski, P. A., Houston, G. C., Krestin, G. P., & van
863 der Lugt, A. (2007). Fiber density asymmetry of the arcuate fasciculus in relation to
864 functional hemispheric language lateralisation in both right-and left-handed healthy
865 subjects: a combined fMRI and DTI study. *Neuroimage*, 35(3), 1064-1076.
- 866
867 Vingerhoets, G., Verhelst, H., Gerrits, R., Badcock, N., Bishop, D. V., Carey, D., ... &
868 LICl consortium. (2023). Laterality indices consensus initiative (LICl): A Delphi expert
869 survey report on recommendations to record, assess, and report asymmetry in
870 human behavioural and brain research. *Laterality*, 28(2-3), 122-191.
- 871
872 Walenski, M., Europa, E., Caplan, D., & Thompson, C. K. (2019). Neural networks
873 for sentence comprehension and production: An ALE-based meta-analysis of
874 neuroimaging studies. *Human brain mapping*, 40(8), 2275-2304.
- 875
876 Wegrzyn, M., Mertens, M., Bien, C. G., Woermann, F. G., & Labudda, K. (2019).
877 Quantifying the confidence in fMRI-based language lateralisation through laterality
878 index deconstruction. *Frontiers in Neurology*, 10, 655.
- 879

- 880 Westerhausen, R., Kreuder, F., Sequeira, S. D. S., Walter, C., Woerner, W., Wittling,
881 R. A., ... & Wittling, W. (2006). The association of macro-and microstructure of the
882 corpus callosum and language lateralisation. *Brain and language*, 97(1), 80-90.
883
- 884 Yeh, F. C., Wedeen, V. J., & Tseng, W. Y. I. (2010). Generalized q -sampling
885 imaging. *IEEE transactions on medical imaging*, 29(9), 1626-1635.
886
- 887 Yeh, F. C., & Tseng, W. Y. I. (2011). NTU-90: a high angular resolution brain atlas
888 constructed by q-space diffeomorphic reconstruction. *Neuroimage*, 58(1), 91-99.
889
- 890 Yeh, F. C., Verstynen, T. D., Wang, Y., Fernández-Miranda, J. C., & Tseng, W. Y. I.
891 (2013). Deterministic diffusion fiber tracking improved by quantitative
892 anisotropy. *PloS one*, 8(11), e80713.
893
- 894 Yeh, F. C., Badre, D., & Verstynen, T. (2016). Connectometry: a statistical approach
895 harnessing the analytical potential of the local connectome. *Neuroimage*, 125, 162-
896 171.
897
- 898 Yeh, F. C., Panesar, S., Barrios, J., Fernandes, D., Abhinav, K., Meola, A., &
899 Fernandez-Miranda, J. C. (2019). Automatic removal of false connections in diffusion
900 MRI tractography using topology-informed pruning (TIP). *Neurotherapeutics*, 16, 52-
901 58.
902
- 903 Yeh, F. C., Panesar, S., Fernandes, D., Meola, A., Yoshino, M., Fernandez-Miranda,
904 J. C., ... & Verstynen, T. (2018). Population-averaged atlas of the macroscale human
905 structural connectome and its network topology. *Neuroimage*, 178, 57-68.
906
- 907 Yeh, F. C. (2020). Shape analysis of the human association
908 pathways. *Neuroimage*, 223, 117329.
909
- 910 Zhong, A. J., Baldo, J. V., Dronkers, N. F., & Ivanova, M. V. (2022). The unique role
911 of the frontal aslant tract in speech and language processing. *NeuroImage:
912 Clinical*, 34, 103020.

913
914
915 Figure and table legends:

916
917 **Figure 1.** Regions of interest (ROIs) were selected to calculate LQ based on Jaccard-
918 Tanimoto index (more details provided in text) (Seghier et al., 2019). The LQ value is
919 expressed as a percentage, ranging from -1 to 1. Values greater than 1/3 indicate left-
920 lateralization, values less than -1/3 indicate right-lateralization, and values between -1/3 and
921 1/3 indicate bilateral orientation (Seghier et al, 2019). TE1 – temporal area 1, found in middle
922 temporal gyrus; STS – superior temporal sulcus; STG – superior temporal gyrus; TG –
923 temporal gyrus; TE2 – temporal area, including ventral and dorsal parts of inferior temporal
924 gyrus.

925 **Figure 2.** Flowchart of the methods pipeline. The pre-processed diffusion MRI data was
 926 reconstructed in an MNI space. The outputs of the reconstruction and SDFs were calculated
 927 to obtain the fibre orientations using DSI studio. Then, two different approaches were used
 928 to examine the white matter tracts associated with language laterality. The connectometry
 929 approach involved obtaining a local connectome matrix and finding out its association with
 930 LQ. Shape analysis involved the recognition of the WM tracts using HCP atlas and mapping
 931 eleven WM fibre bundles important for language function. The measures of key shape
 932 features, such as curl and volume, were extracted and linear regression analyses were used
 933 to look at the associations between shape metrics and LQ.

934 **Figure 3.** Eleven white matter tracts were reconstructed for shape analysis based on the
 935 HCP842 atlas computed on 1065 healthy people (Yeh et al, 2018).

936 **Figure 4.** Schematic illustration of the shape analysis of the white matter tracts. (a) The area
 937 metrics used in the included surface area (mm). (b) The length metrics used in the study
 938 included mean tract length (mm) as well as span bundle (mm) and diameter (mm) of the
 939 bundle. (c) The volume metrics used in the study included branch volume (mm³) (blue
 940 dotted line), trunk volume (mm³) (right dotted line), and total bundle volume (mm³) (black
 941 dotted line) (d) The shape metrics used in the study included curl and elongation.

942 **Figure 5.** Cohen's d maps of language comprehension task. The colour bar indicates Z
 943 scores; L – left hemisphere; R – right hemisphere.

944 **Figure 6.** Connectometry results for the language lateralisation in frontal lobe (n=1040). a)
 945 Tract sections negatively correlated with LQ ($p < 0.01$, FDR corrected). b) Tract sections
 946 positively correlated with LQ ($p < 0.01$, FDR corrected). Abbreviations: CC, corpus callosum.
 947 Colour bar represents t-statistic. See Extended Figure 6-1 for the group level posthoc
 948 analyses.

949 **Figure 7.** Connectometry results for the language lateralisation in temporal lobe (n=1040). a)
 950 Tract sections negatively correlated with LQ ($p < 0.01$, FDR corrected). b) Tract sections
 951 positively correlated with LQ ($p < 0.01$, FDR corrected). Abbreviations: AF -arcuate
 952 fasciculus; CC, corpus callosum; CS – corticospinal; DRT - dentatorubrothalamic. Colour bar
 953 represents t-statistic. See Extended Figure 7-1 for the group level posthoc analyses.

954 **Figure 8.** Violin plots (right) illustrating the mean length distribution in (a) the right IFOF and
 955 (b) the forceps minor (illustrated in left), across different temporal language lateralisation
 956 groups. Group differences are analysed using Tukey post-hoc tests, with adjustments for
 957 FDR. Significant differences are indicated by p-values less than 0.05 (FDR corrected), while
 958 non-significant differences are denoted by p-values greater than 0.05 (FDR corrected).

959

960 **Table 1.** A list of abbreviations used in this article.

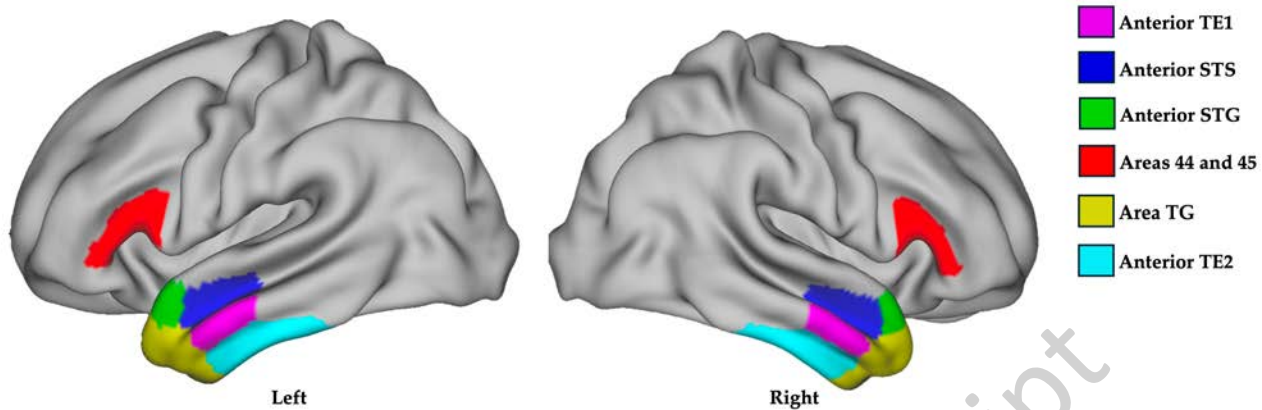
Abbreviation	Definition
AF	Arcuate Fasciculus
ANOVA	Analysis of Variance
BLR	Bilateral Language Representation
BOLD	Blood-Oxygen-Level-Dependent Signal
CIFTI	Connectivity Informatics Technology Initiative Grayordinate Space
COPE	Contrast Of Parameter Estimates (COPE) Map
FDR	False Discovery Rate
FAT	Frontal Aslant Tract
FNIRT	a "medium resolution" non-linear registration method
FSL	The FMRIB Software Library
FWE	Family-Wise Error
fMRI	Functional Magnetic Resonance Imaging
HCP	Human Connectome Project
HLD	Hemispheric Language Dominance
IFOF	Inferior Fronto-Occipital Fasciculus
ILF	Inferior Longitudinal Fasciculus
LLD	Left Language Dominance
LQ	Laterality Quotient
MNI	Montreal Neurological Institute Space
MSM-ALL	Multimodal Surface Matching Registration
MSM-SULC	Cortical Folding-Based Registration
QA	Quantitative Anisotropy
ROI	Region Of Interest
RLD	Right Language Dominance
SDF	Spin Distribution Function

SLF	Superior Longitudinal Fasciculus
STGa	Superior Temporal Gyrus anterior
STSda	Superior Temporal Sulcus dorsal anterior
STSva	Superior Temporal Sulcus ventral anterior
TE1a	Temporal Area 1 anterior
TE2a	Temporal Area 2 anterior
TGd	Temporal Gyrus dorsal
TGv	Temporal Gyrus ventral

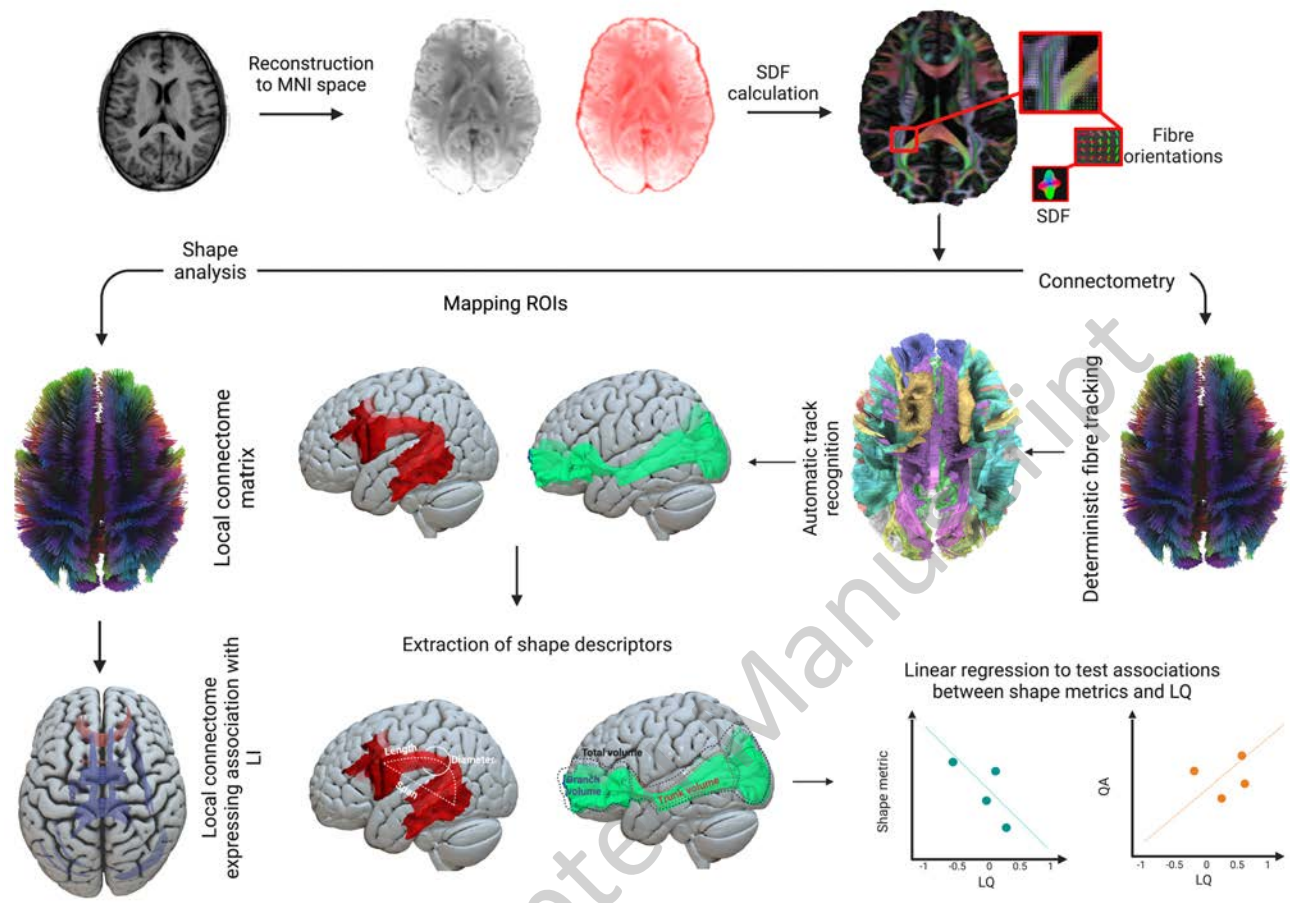
961

962

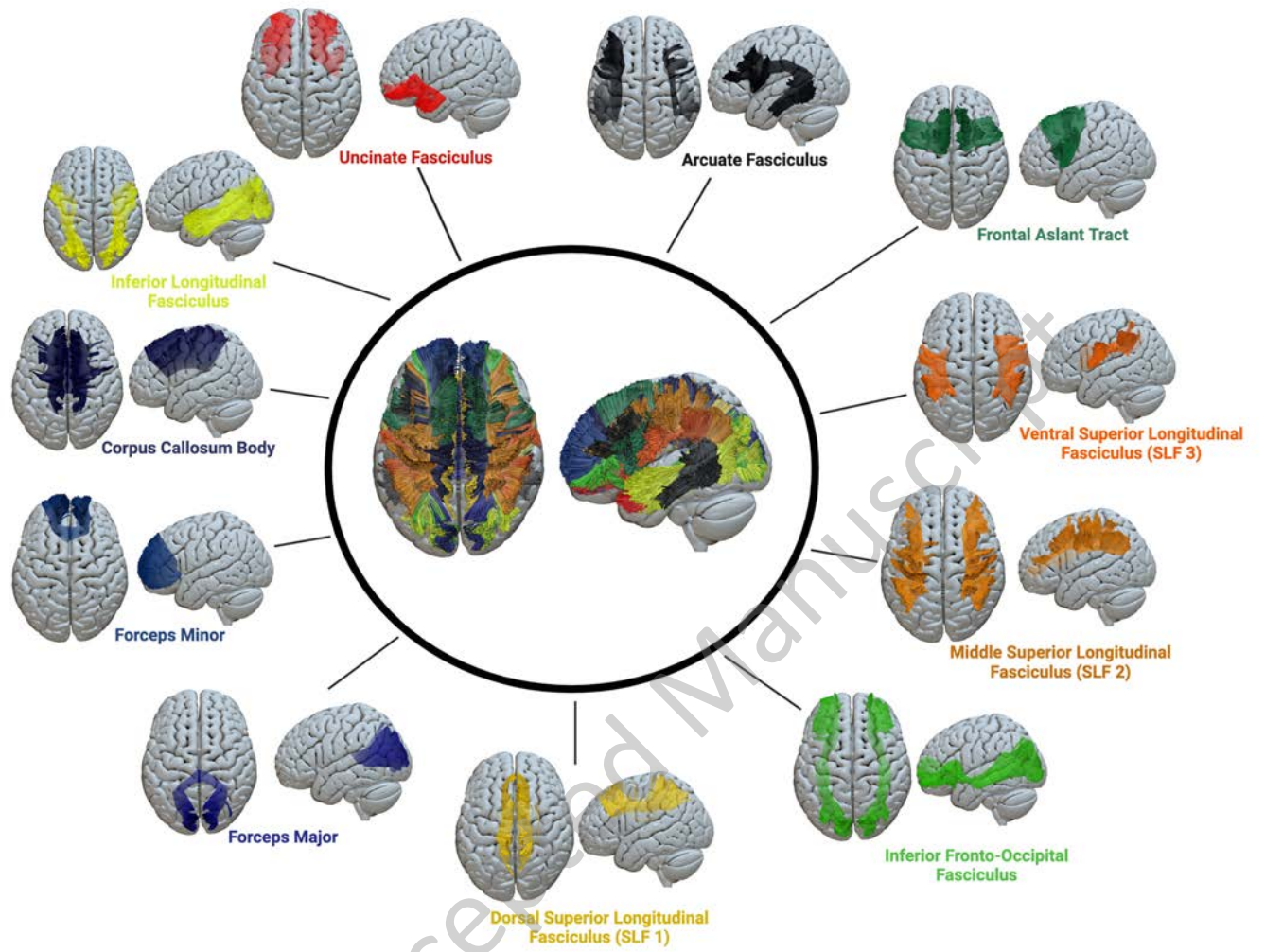
JNeurosci Accepted Manuscript



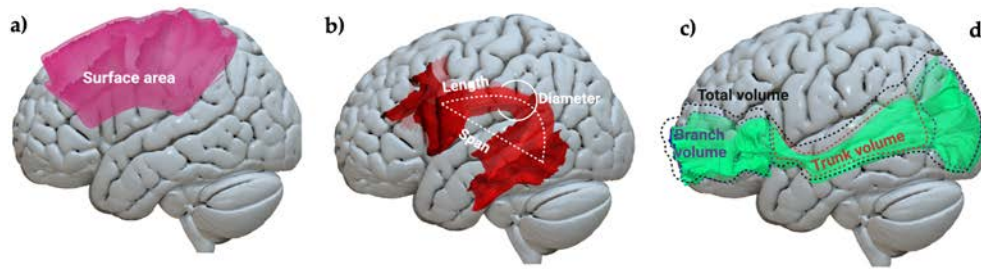
JNeurosci Accepted Manuscript



JNeurosci Accepted Manuscript

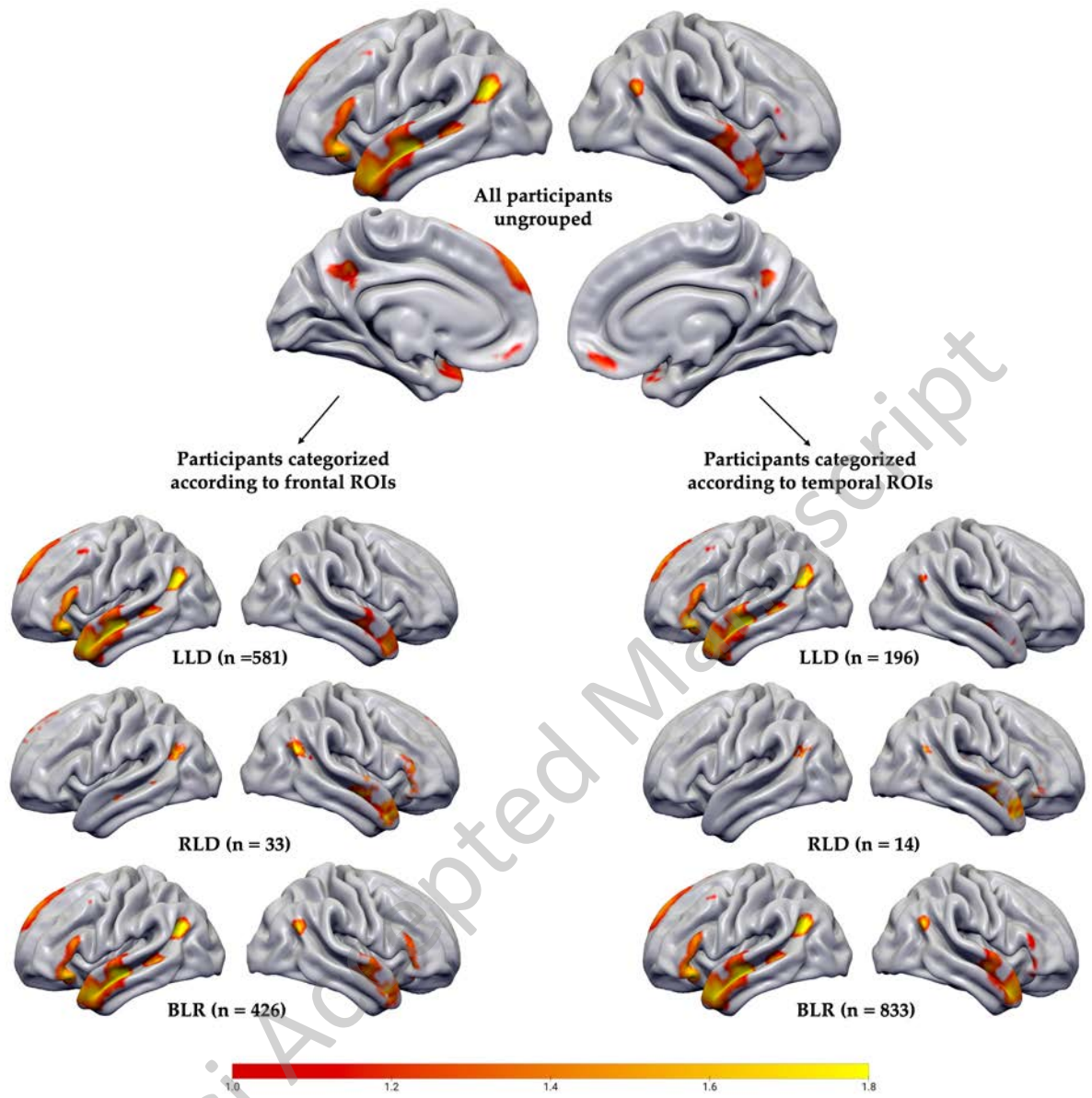


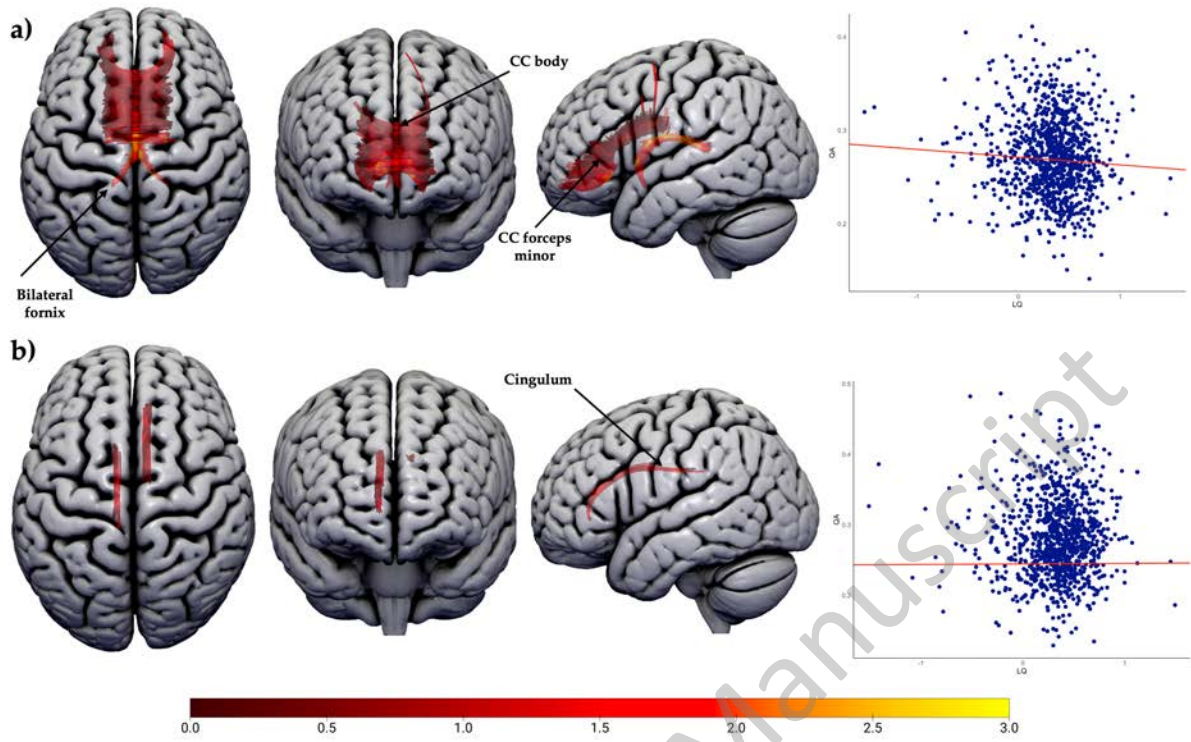
JNeurosci Accepted Manuscript



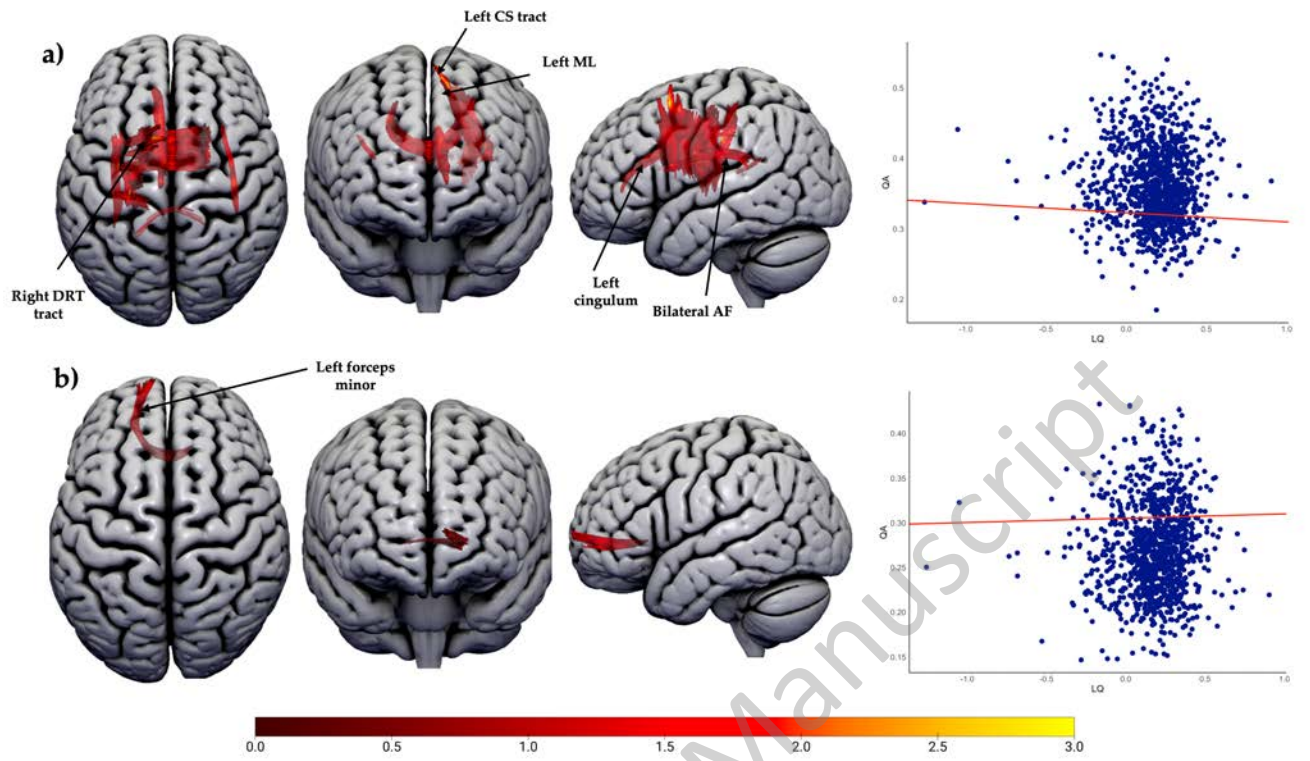
$$Curl = \frac{length}{span}$$
$$Elongation = \frac{length}{diameter}$$

JNeurosci Accepted Manuscript

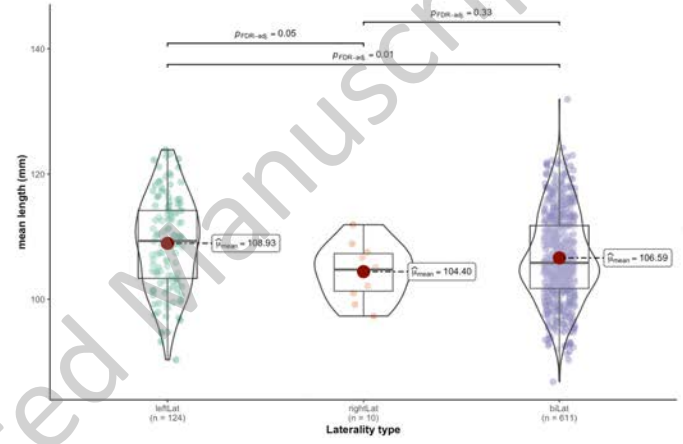
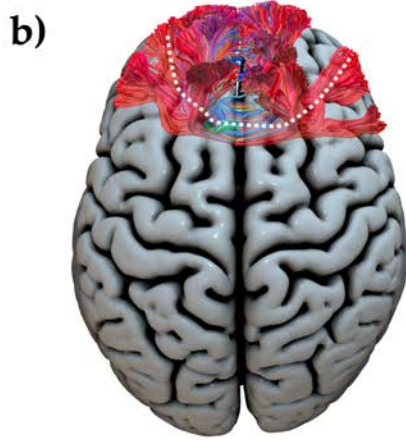
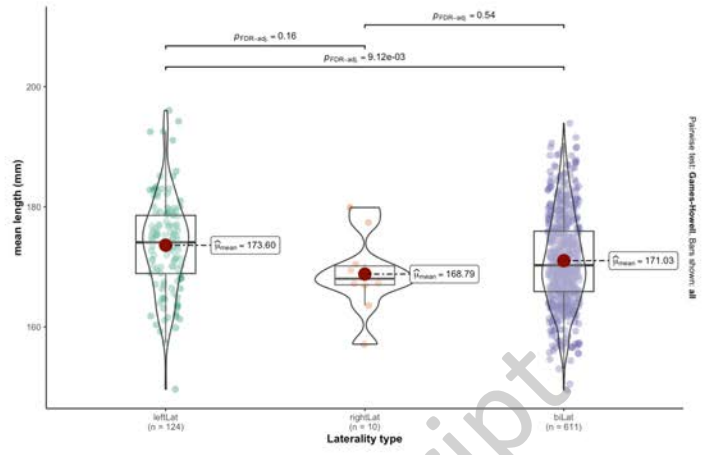
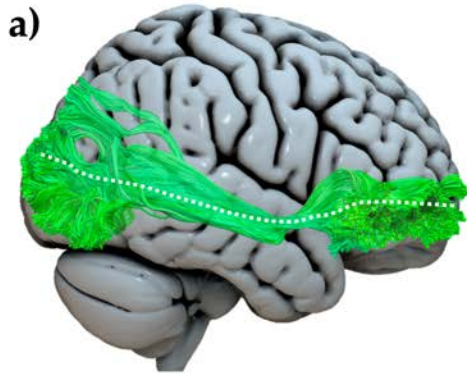




JNeurosci Accepted Manuscript



JNeurosci Accepted Manuscript



JNeurosci Accepted Manuscript